A. H. A. El-Beik
Department of Civil and Structural Engineering
University of Manchester Institute of Science and Technology
Manchester M60 1QD, England
R. Babaei-Mahani†
Engineering Department (Simon Engineering Laboratory)
University of Manchester
Manchester M13 9PL, England

The Quadrustational Close-Range Photogrammetric System*

A greater and more homogeneous accuracy is attained when four, rather than two, camera stations are employed.

Introduction

The development of the stereometric camera was a significant event in close-range photogrammetry and is reviewed in detail by Karara (1974). The data reduction using single or stereo geometry and the study of the accuracy of both systems has attracted the attention of many photogrammetrists, including Thompson (1971), Abdel-Aziz and Karara (1971), Faig (1972), and Wong (1975). In an attempt to reduce the degree of uncertainty by allowing double checking, a quadrustational close-range photogrammetric system has been developed.

Abstract: *Mathematical models representing the geometry of a quadrustational close-range photogrammetric system were developed using the optimization from rays and planes to determine the optimal point of intersection. The system was verified for the normal case using a multistation/multistereo configuration. The accuracy of the system was assessed by taking stereocomparator measurements from stereopairs of a specially constructed controlled field.*

The results of experimental studies revealed that (a) the accuracy in all coordinate axes is more homogeneous when using the quadrustational system, as compared with the conventional two-station system; and (b) The quadrustational system produces greater accuracy in the Z-dimension (parallel to the camera optical axis) than does the conventional system.

In developing such a system, the following points were taken into consideration:

- that the system should be a versatile one, to be used for stereo as well as multi-stereo;
- that the system should be easily adapted for the normal as well as the general case of close-range photogrammetry;
- that the assembly of the data acquisition system and its operation should be simple and the apparatus, if possible, portable;
- that mathematical expressions should be derived for both the normal case and the general case using a strong geometric representation for the data reduction system; and
- that a special test board should be designed and precisely constructed, so that a comparison could be made between the results obtained from the stereo and multi-stereo systems.

The system described in this paper is based on four stations only, and the mathematical models representing its geometry were developed. The system was verified using a data reduction system based on a digitized Zeiss Jena Steko 1818 stereocomputer.

Configuration of the System

The configuration of the system which would conform with most of the requirements listed in the introduction is illustrated in Figure 1. The system is based on four camera stations located at the corners of a quadrangle. The quadrangle can take the shape of a square or a rectangle, depending on the design of the data acquisition system.

* Presented paper, Commission V of the International Society for Photogrammetry and Remote Sensing, Symposium at York, UK (5-10 September 1982).

† Presently with the Department of Civil Engineering, The City University, London, England.

Photogrammetric Engineering and Remote Sensing,
Vol. 50, No. 3, March 1984, pp. 319-326.

0099-1112/84/5003-0319$02.25/0

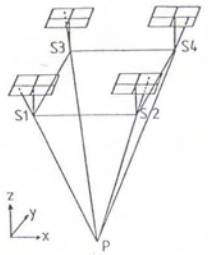

FIG. 1. Intersection of rays in quadrustational geometry.

Ideally, the number of photogrammetric cameras required for this system is four. In this experiment only static objects were considered, and as a result, due to the excessively high cost involved, it was decided to use two cameras only which can be mounted on an adjustable stereometric stand (Figure 2). Such a configuration is easily achieved with little or no modification to the stereometric camera system. The four-station system can be achieved by raising the stereometric frame to the required height (Figure 2). Due to the configuration of the four stations, the system is named the "quadrustational" close-range photogrammetric system and is referred to as the quadrustational system in the various parts of the paper.

The system used in this experiment consists of a specially designed stereometric stand and two UMK 10/1318 short-range cameras (1.5 m to 4.4 m). The stereometric stand (Figure 2) was made in such a way that the optical axes of each camera can be inclined in the X and Y directions. A hydraulic jack is

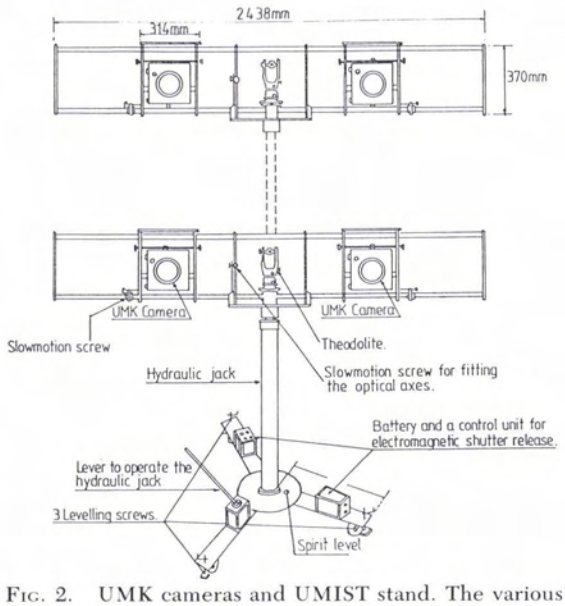

FIG. 2. UMK cameras and UMIST stand. The various components of the stereometric system and the manner in which the quadrustational system is achieved is indicated.

incorporated into the system to allow the formation of quadrustational photography. The object to be measured is first photographed from position S_1 and S_2 (Figure 1); then the horizontal frame upon which the cameras are mounted is raised to position S_3 and S_4 and a second stereopair is taken. Throughout this paper, the camera stations are referred to as S_1, S_2, S_3, and S_4. Stereopairs are referred to by the two stations involved in each particular pair.

Quadrustational Geometry

Considering Figure 1, and assuming that all rays intersect with each other at a point $P(X_p, Y_p, Z_p)$, then the equation of each ray $\mathbf{R}_i$ is

$$\begin{pmatrix} X_p \\ Y_p \\ Z_p \end{pmatrix} = \begin{pmatrix} X_{s_i} \\ Y_{s_i} \\ Z_{s_i} \end{pmatrix} + \lambda_i \begin{pmatrix} X_{R_i} \\ Y_{R_i} \\ Z_{R_i} \end{pmatrix} \tag{1}$$

or

$$\mathbf{X} = \mathbf{S}_i + \boldsymbol{\lambda}_i \mathbf{R}_i \tag{2}$$

where i varies from 1 to 4 for the quadrustational system, giving 12 equations.

By eliminating λ_i between these equations, the following equations are obtained:

$$\begin{aligned}
&(X_{s_2} - X_{s_1})\,Z_{R_2} - (Z_{s_2} - Z_{s_1})\,X_{R_2} + A\,(Z_{R_1}X_{R_2} - X_{R_1}Z_{R_2}) = 0 \\
&(X_{s_3} - X_{s_1})\,Y_{R_3} - (Y_{s_3} - Y_{s_1})\,X_{R_3} + A\,(Y_{R_1}X_{R_3} - X_{R_1}Y_{R_3}) = 0 \\
&(X_{s_3} - X_{s_1})\,Z_{R_3} - (Z_{s_3} - Z_{s_1})\,X_{R_3} + A\,(Z_{R_1}X_{R_3} - X_{R_1}Z_{R_3}) = 0 \\
&(X_{s_4} - X_{s_1})\,Y_{R_4} - (Y_{s_4} - Y_{s_1})\,X_{R_4} + A\,(Y_{R_1}X_{R_4} - X_{R_1}Y_{R_4}) = 0 \\
&(X_{s_4} - X_{s_1})\,Z_{R_4} - (Z_{s_4} - Z_{s_1})\,X_{R_4} + A\,(Z_{R_1}X_{R_4} - X_{R_1}Z_{R_4}) = 0
\end{aligned} \tag{3}$$

where

$$A = \frac{(Y_{s_2} - Y_{s_1})X_{R_2} - (X_{s_2} - X_{s_1})Y_{R_2}}{Y_{R_1}X_{R_2} - X_{R_1}Y_{R_2}}$$

in which X_{R_i}, Y_{R_i}, Z_{R_i} $(i = 1,2,3,4)$ are components of the vector $\mathbf{R}_i$ and are obtained from

$$\mathbf{R}_i = \lambda_i' \mathbf{M}^{\mathrm{T}}{}_i \mathbf{r}_i$$

where λ_i' is the scale factor of location vector $\mathbf{r}_i$ in the image system and $\mathbf{M}_i$ is the rotation matrix.

The equation can further be reduced by taking the rotations at all stations relative to the lower left station S_1 (Figure 1), so that $\mathbf{R}_1 = \mathbf{I}$ (unit matrix).

Equations 3 are nonlinear and must be transformed to a linear set of equations. Using a Taylor series expansion and neglecting second and higher order terms, we obtain the following linearized observation equations:

$$F_i = F_1^{\circ} + \frac{\partial F_i}{\partial u_i} \tag{4}$$

where, in the case of the reduced form,

$$u_i = \mathrm{f}\,(B_{x_i},\ i = 2,3,\ B_{y_i},\ B_{z_i},\ i = 1,2,3,\ \omega_i,\ \phi_i,\ \kappa_i,\ i = 2,3,4).$$

The B's are base components and are given by

$$\mathbf{B} = \begin{pmatrix} B_{x_i} \\ B_{y_i} \\ B_{z_i} \end{pmatrix} = \begin{pmatrix} X_{s_{i+1}} - X_{s_1} \\ Y_{s_{i+1}} - Y_{s_1} \\ Z_{s_{i+1}} - Z_{s_1} \end{pmatrix} \tag{5}$$

The solution of the n Equations 4 then gives approximate values of the unknowns (dB_{x_i}, dB_{y_i}, . . . , dK_i), which are then added to the initial approximations to obtain a further iterative solution. Usually, for four or more control points, the solution is obtained using a least-squares procedure.

As the object space coordinates are not included in Equation 3, the solution of Equation 3 is based on relative orientation only.

In order to meet the control requirement, the collinear model which involves the reference position of object points was also used in this experiment. The quadrustational system (Figure 1) is expressed by considering four central projections of points in a three-dimensional object space onto four image planes. These conditions can be expressed mathematically for the ith photograph as

$$\begin{aligned} x_i\,\mathbf{M}_3^i\,\overline{\mathbf{X}_i} + f_i\,\mathbf{M}_1^i\,\overline{\mathbf{X}_i} &= 0 \\ y_i\,\mathbf{M}_3^i\,\overline{\mathbf{X}_i} + f_i\,\mathbf{M}_2^i\,\overline{\mathbf{X}_i} &= 0 \end{aligned} \tag{6}$$

where

$$\mathbf{M}_i = \begin{pmatrix} \mathbf{M}_1^i \\ \mathbf{M}_2^i \\ \mathbf{M}_3^i \end{pmatrix} \text{ and } \mathbf{M}_j^i = [m_{j1}^i\ m_{j2}^i\ m_{j3}^i]\ j = 1,2,3$$

$$\overline{\mathbf{X}_i} = \begin{pmatrix} X_p - X_{S_i} \\ Y_p - Y_{s_i} \\ Z_p - Z_{S_i} \end{pmatrix} \text{ for each } i,\ p = 1, 2, \ldots, N \text{ control points}$$

The two expressions (Equation 6) are nonlinear, and the same principle of linearization as stated before may be used.

With the quadrustational system, there are 24 unknowns (elements of exterior orientation for each camera station).

Because each control point yields eight observation equations (two for each ray), then with a minimum of three control points a unique solution is possible. For four or more control points, a least-squares procedure is used.

Determination of Spatial Coordinates

Once the coordinates of the camera exposure stations and their orientation have been established, the spatial coordinates of new points on the object may be determined.

In this section, two different procedures are developed, both being based on the determination of an optimum point to represent the intersection.

In the first approach, the volume of the tetrahedron formed by the mutual intersection of the four rays (Figure 1) is minimized. In the second approach the same procedure is employed but four planes (four sides as in Figure 1) instead of rays are used.

Optimization using rays

Referring to Figure 3, the four rays $\mathbf{R}_i$ (i = 1,2,3,4) could fail to intersect at one point; thus, a mathematical model must be developed to obtain an optimum point. Figure 4 shows only one of these rays. If p is the optimum point, then

$$\mathbf{T}_i p \cdot \mathbf{S}_i\,\mathbf{T}_i = 0 \tag{7}$$

and

$$\mathbf{T}_i p = u_i j_i = \mathbf{S}_i p - \mathbf{S}_i \mathbf{T}_i,\ i = 1,2, \ldots, N;$$

therefore,

$$(\mathbf{S}_i p - \mathbf{S}_i \mathbf{T}_i) \cdot \mathbf{S}_i \mathbf{T}_i = 0$$

or

$$\mathbf{S}_i p \cdot \mathbf{S}_i \mathbf{T}_i = (\mathbf{S}_i \mathbf{T}_i);^2$$

Assuming l_i, m_i, n_i are direction cosines of $\mathbf{S}_i\mathbf{T}_i$; then

$$(X - X_i,\ Y - Y_i,\ Z - Z_i)\ \lambda_i (l_i, m_i, n_i)^{\mathrm{T}} = \lambda_i^2. \tag{8}$$

Hence

$$\lambda_i = (X - X_i)\ l_i + (Y - Y_i) m_i + (Z - Z_i) n_i$$

Also

$$u_i^2 = (S_i p)^2 - \lambda_i^2 \tag{9}$$

or

$$\begin{aligned} u_i^2 = {} & (X - X_i)^2 + (Y - Y_i)^2 + (Z - Z_i)^2 \\ & - (X - X_i)^2\, l_i^2 - (Y - Y_i)^2 m_i^2 \\ & - (Z - Z_i)^2 n_i^2 \\ & - 2(X - X_i)(Y - Y_i) l_i m_i \\ & - 2(X - X_i)(Z - Z_i)\ l_i n_i \\ & - 2(Y - Y_i)(Z - Z_i) m_i n_i \end{aligned} \tag{10}$$

Assuming

$$\sigma = \sum_{i=1}^{4} u_i^2 \tag{11}$$

and differentiating σ with respect to X, Y, and Z, we get

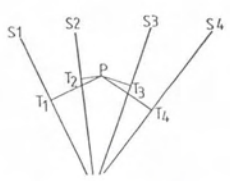

Fig. 3. Four rays in space and the optimum point, P.

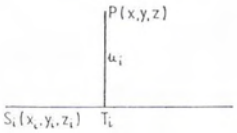

FIG. 4. The perpendicular to one of the rays in the quadrustational system.

$$\begin{pmatrix} a_{11} & a_{12} & a_{13} \\ a_{12} & a_{22} & a_{23} \\ a_{13} & a_{23} & a_{33} \end{pmatrix} \begin{pmatrix} X \\ Y \\ Z \end{pmatrix} = \begin{pmatrix} b_{11} \\ b_{21} \\ b_{31} \end{pmatrix} \tag{12}$$

where

$$a_{11} = \sum_{i=1}^{4} (1 - l_i^2)$$

$$a_{12} = \sum_{i=1}^{4} l_i m_i$$

$$a_{13} = \sum_{i=1}^{4} l_i n_i$$

$$a_{23} = \sum_{i=1}^{4} n_i m_i$$

$$a_{22} = \sum_{i=1}^{4} (1 - m_i^2)$$

$$a_{33} = \sum_{i=1}^{4} (1 - n_i^2)$$

$$b_{11} = \sum_{i=1}^{4} \{(1 - l_i^2)X_i - l_i m_i Y_i - l_i n_i Z_i\}$$

$$b_{21} = \sum_{i=1}^{4} \{- l_i m_i X_i + (1 - m_i^2)Y_i - m_i n_i Z_i\}$$

$$b_{31} = \sum_{i=1}^{4} \{- l_i n_i X_i - m_i n_i Y_i - (1 - n_i^2)Z_i\}$$

The direction cosines used in Equation 12 are obtained by using the image coordinate system (Figure 5) and the rotation matrix **M**.

The direction cosines of a line from the exposure station to the image point are

$$\frac{S_i a_i}{d_i} = \begin{pmatrix} \cos \alpha_i \\ \cos \beta_i \\ \cos \gamma_i \end{pmatrix} = \begin{pmatrix} -x_i/d_i \\ -y/d_i \\ f/d_i \end{pmatrix} \tag{13}$$

where

a_i = the image point
S_i = ith exposure station

and

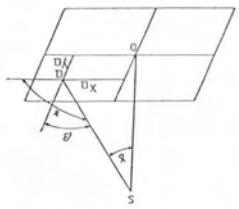

FIG. 5. Image coordinate system.

$$d_i = (x_i^2 + y_i^2 + f_i^2)^{1/2}$$

Then the direction cosines of the line from exposure station S to the object-point A is

$$S_i A_i = \mathbf{M}_i^{\mathrm{T}} S_i a_i$$

or

$$\begin{pmatrix} l_i \\ m_i \\ n_i \end{pmatrix} = \mathbf{M}_i^{\mathrm{T}} \begin{pmatrix} \cos \alpha_i \\ \cos \beta_i \\ \cos \gamma_i \end{pmatrix} \tag{14}$$

The matrix of coefficients in Equation 12 is symmetrical, and the solution is obtained from these three linear equations. This newly developed procedure can be used for any data acquisition system configuration based on more than two stations.

OPTIMIZATION USING PLANES

The second method of obtaining the spatial coordinates is based on optimization using the planes at the four sides of the quadrustational pyramid (Figure 1). However, it should be emphasized that this method cannot be used for a two-station system.

The general equation of a plane in the system is given by the following equation:

$$\begin{pmatrix} X - X_{s_i} & Y - Y_{s_i} & Z - Z_{s_i} \\ X_{R_i} & Y_{R_i} & Z_{R_i} \\ BX_i & BY_i & BZ_i \end{pmatrix} = 0 \tag{15}$$

Expanding Equation 15 we get

$$A_i X + B_i Y + C_i Z + D_i = 0 \tag{16}$$

where

$$A_i = (YR_i BZ_i - ZR_i BY_i)$$
$$B_i = -(XR_i BZ_i - ZR_i BX_i)$$
$$C_i = (XR_i BY_i - YR_i BX_i)$$
$$D_i = -\begin{pmatrix} X_{s_i} & Y_{s_i} & Z_{s_i} \\ X_{R_i} & Y_{R_i} & X_{R_i} \\ BX_i & BY_i & BZ_i \end{pmatrix}$$

The length of perpendicular line from the optimum point (X_p, Y_p, Z_p) to each plane is

$$L_i = \frac{A_i X_p + B_i Y_p + C_i Z_p - D_i}{\sqrt{T_i}} \tag{17}$$

where

$$T_i = A_i^2 + B_i^2 + C_i^2.$$

We assume that

$$\sigma = \sum_{i=1}^{4} L_i^2. \tag{18}$$

then, by minimizing σ, we get

$$\frac{\partial\sigma}{\partial X_p} = \frac{\partial\sigma}{\partial Y_p} = \frac{\partial\sigma}{\partial Z_p} = 0 \tag{19}$$

Equation 19 can be written in the following form:

$$\sum_{i=1}^{4} \frac{1}{T_i} \begin{pmatrix} A_i^2 & A_iB_i & A_iC_i \\ A_iB_i & B_i^2 & B_iC_i \\ A_iC_iB_iC_i & C_i^2 & \end{pmatrix} \begin{pmatrix} X_p \\ Y_p \\ Z_p \end{pmatrix} = \sum_{i=1}^{4} \frac{1}{T_i} \begin{pmatrix} A_iD_i \\ B_iD_i \\ C_iD_i \end{pmatrix}. \tag{20}$$

Again, the coefficient matrix is symmetrical, and the optimum point is obtained by solution of these linear equations.

The Normal Case of the Quadrustational System

In addition to the generalized geometry described in the previous sections, it was also decided to verify the results using the geometry based on the normal case.

Considering Figure 1, and extending the basic parallax equation, the third dimension, Z, for the whole system is given by

$$Z = H + B/4 \left[\frac{1}{K_{x_2} - K_{x_1}} + \frac{1}{K_{x_4} - K_{x_3}} - \frac{1}{K_{x_5}} - \frac{1}{K_{x_6}} \right] \tag{21}$$

where

$$K_{x_i} = \frac{x_i}{f_i}, \ (i = 1,2,3,4), \ K_{x_5} = \frac{p_1}{f_1} \text{ and } K_{x_6} = \frac{p_2}{f_2}$$

and

H is the camera-object distance;

B is the camera base;

f_1, f_2 are the principal distances of the two cameras; and

p_1 and p_2 are the values of parallax (parallax in the direction of the base) measured on stereopairs $S_1 - S_3$ and $S_2 - S_4$ and are given by

$$p_1 = y_1 - y_3$$
$$p_2 = y_2 - y_4$$

Equation 21 is based on the special symmetrical case, in which the system has all four cameras at equal separations.

Equation 21 gives the height of the object above the selected datum. The X and Y coordinates can be found by using the basic parallax equation.

Experimental Study

In order to verify the practicability and to investigate the resulting accuracy of the quadrustational system, a series of tests were carried out. In all experiments, the two short-range UMK cameras referred to before were used for data acquisition. A digitized Zeiss Jena Steko 1818 stereocomparator was used for measurements, and data were processed using CYBER and facilities of UMRCC (University of Manchester Regional Computer Centre). In order to fulfill the control requirements, a precise control field was constructed and is described in the following section.

Control Field

In order to have all measurements related to the same datum plane, it is essential to provide a precise control field containing well-distributed control points. The control field used in this experiment is a permanent field which is fixed on a vertical wall. It consists of a metal sheet, two metres long by one metre wide, fixed on a wooden board of the same size. A 20 cm by 20 cm grid network was drawn on the metal sheet. Forty-eight columns of different length were made from aluminium bars, and a magnet was fixed in a hole at the base of each column (Figure 6). This arrangement was made in order to allow for changes in the position of control points and also to place them accurately on any grid point desired. The grid points were numbered from 1 to 10 horizontally and from A to E vertically. Crosses also were drawn at corners and midway along the upper and lower sides for horizontal control. The height of the column was measured precisely using a machine called the Conquest International Inspection Machine. The measurements on this machine are based on optical gratings refined by a moiré measuring system which provides a digital readout of the distance moved by the probe in each of three coordinate directions. The resolution of the system is one micrometre. Over each of the three coordinate gratings of the machine runs a unit containing a light source and a subsidiary grating which creates moiré fringes with the main grating.

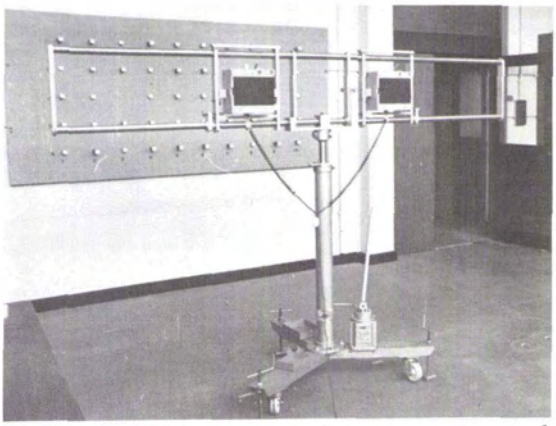

Fig. 6. The UMK cameras on their stereometric stand. The control field is mounted on the wall.

TABLE 1. ROOT-MEAN-SQUARE ERRORS FOR THE NORMAL CASE

Photos	X (mm)	Y (mm)	Z (mm)
S_1–S_2	0.19	0.33	0.58
S_3–S_4	0.24	0.33	0.66
S_1–S_3	0.31	0.21	0.55
S_2–S_4	0.26	0.29	0.68
Aver.	0.25	0.29	0.62
S_1–S_2–S_3–S_4	0.16	0.19	0.28

TABLE 2. ROOT-MEAN-SQUARE ERRORS FOR THE GENERAL CASE

Photos	X (mm)	Y (mm)	Z (mm)
S_1–S_2	0.21	0.31	0.43
S_3–S_4	0.17	0.24	0.51
S_1–S_3	0.26	0.09	0.43
S_2–S_4	0.31	0.29	0.60
Aver.	0.24	0.23	0.49
S_1–S_2–S_3–S_4	0.17	0.15	0.26

The sinusoidal output is subdivided into levels which in turn are counted and displayed by the unit as a measure of the distance traveled by the probe in the direction of each coordinate.

Because of the large size of the control field, the plane measurement of the crosses was not possible directly on this machine. Therefore, the measurement of the crosses was checked against a bar of 1.5-m length, which was precisely graduated using the projection microscope of the Conquest machine.

DATA ACQUISITION AND DATA REDUCTION

The camera stand was set up parallel to the control field, with the camera axis perpendicular to the base. A one-second theodolite was used for the orientation of the stereometric stand. Pairs of photographs were taken with the UMK short-range cameras with equal vertical and horizontal bases. Measurements were taken on stereopairs S_1-S_2, S_3-S_4, S_1-S_3, and S_2-S_4 using the Zeiss Jena Steko 1818 stereocomparator.

RESULTS

Test 1. The normal case of the quadrustational system. The average RMS (root-mean-square) error of 24 points in each stereopair after processing is given in Table 1.

On studying Table 1, it is apparent that the accuracy is fairly consistent in the case of the individual stereopairs, while an improved accuracy is noticeable in the case of the normal case of the quadrustational system. In the *X*-direction an improvement of 36 percent, in the *Y*-direction an improvement of 14.5 percent, and in the *Z*-direction an improvement of 54.8 percent has been achieved using the geometry of the quadrustational system. So it is clear that the normal case of the quadrustational system has provided a substantial increase in the accuracy, with its highest value in the Z direction, the accuracy of which is of vital importance in most engineering applications.

Test 2. The general case of the quadrustational system. Some of the photographs which were used for the normal case were measured and solved using the general case. The RMS errors for each stereopair and also for the quadrustational system are given in Table 2.

On studying the results presented in Table 2, it is noticeable that the use of the quadrustational system improved the accuracy by 28.4 percent in the *X*-direction, by 34.4 percent in the *Y*-direction, and by 47.2 percent in the *Z*-direction.

Test 3. The general case with equal vertical and horizontal bases. In this test, photographs were taken simultaneously at stations S_1-S_2 and S_3-S_4. The test was carried out for a number of cases throughout the full focusing range of the short-range UMK cameras with a base-to-object distance of 0.5. A theodolite was used to set up the camera stand in front of the control field (as described in the previous section) with respect to the base line. The collinear model was used for resection and orientation. The optimal intersection point was calculated according to the least-squares criterion. The root mean square errors for each focusing distance are given in Table 3.

TABLE 3. ROOT-MEAN-SQUARE ERRORS FOR EACH FOCUSING DISTANCES

Focusing distance (m)	X (mm)		Y (mm)		Z (mm)	
	S_1–S_2	Quadru-stational	S_1–S_2	Quadru-stational	S_1–S_2	Quadru-stational
1.5	0.29	0.21	0.14	0.17	0.29	0.17
1.7	0.34	0.20	0.26	0.11	0.41	0.23
2.6	0.36	0.36	0.43	0.31	0.51	0.08
3.3	0.17	0.29	0.33	0.16	0.34	0.29
4.4	0.26	0.33	0.50	0.41	0.53	0.26

TABLE 4. AVERAGE ROOT-MEAN-SQUARE ERRORS OF THE QUADRUSTATIONAL SYSTEM WITH DIFFERENT BASE TO OBJECT-DISTANCE RATIOS

	RMS		
B/H	X (mm)	Y (mm)	Z (mm)
0.4	0.13	0.16	0.09
0.6	0.10	0.14	0.09
0.8	0.21	0.17	0.19
1.0	0.26	0.13	0.14

The results in Table 3 reveal that the accuracy has been improved in the Z-direction at all focusing distances in the case of the quadrustational system when it is compared with the results of stereopair S_1-S_2. The percentage of improvement of the accuracy in the Z-coordinate is 41 percent, 44 percent, 84 percent, 15 percent, and 51 percent for the abovementioned focusing distances, respectively. However, the results in the X-direction do not show a consistent improvement while in the Y-direction the accuracy has generally been improved.

Test 4T. The quadrustational system with different base to object-distance ratios. In this test photographs were taken at a distance of 1.5 m. Equal vertical and horizontal bases but with different base to object distance ratios were used. The average root-mean-square errors of 19 points are shown in Table 4.

Although one expects an improvement in accuracy by increasing the base to object-distance ratio, the results of this test showed that the highest accuracy is obtained at a B/H of 0.6. Comparing the root-mean-square errors at $B/H = 0.6$ with those at $B/H = 1$, it can be found that results at $B/H = 0.6$ are 61 percent in X and 36 percent in Z more accurate than when $B/H = 1$. However, the root-mean-square error in Y is least at $B/H = 1$.

Test 5. The quadrustational system with different bases. Photographs were taken at four stations from distances of 1.5 m and 3.3 m. Equal and different bases were compared in this test, the results of which are given in Table 5. B_1 and B_2 are horizontal and vertical bases, respectively, and are shown in Figure 1.

TABLE 5. ROOT-MEAN-SQUARE ERRORS FOR EQUAL AND DIFFERENT BASES OF THE QUADRUSTATIONAL SYSTEM

Object distance (m)	$B_1/H = 0.5$, $B_2/H = 0.5$			$B_1/H = 0.5$, $B_2/H = 0.3$		
	X (mm)	Y (mm)	Z (mm)	X (mm)	Y (mm)	Z (mm)
1.5	0.13	0.17	0.13	0.19	0.09	0.11
3.3	0.16	0.17	0.14	0.12	0.21	0.16

TABLE 6. ROOT-MEAN-SQUARE ERRORS OF THE QUADRUSTATIONAL SYSTEM WITH DIFFERENT BASES

Object distance (m)	$B_1/H = 0.6$, $B_2/H = 0.6$			$B_1/H = 0.6$, $B_2/H = 0.3$		
	X (mm)	Y (mm)	Z (mm)	X (mm)	Y (mm)	Z (mm)
2.2	0.23	0.18	0.16	0.16	0.21	0.12

From Table 5 a distinct conclusion cannot be drawn as to whether the accuracy would be different with equal and different bases. In an attempt to obtain a specific answer, a second test was carried out at a focusing distance of 2.2 m but with bases $B_1/H = 0.6$ and $B_2/H = 0.3$. The result of this test is given in Table 6.

The results of test 5 show that there is no consistent variation in root-mean-square errors between equal and different bases in the quadrustational system. The authors feel that in using the quadrustational system it might not be necessary to raise the camera frame to the same amount as that of the separation of the cameras. In other words, there is no noticeable difference as to whether the base of the quadrustational pyramid is square or rectangular. However, if the normal case of the quadrustational system is used, one should check that the B/H ratio of the left and right stereopairs does not affect stereo-vision on the stereocomparator.

CONCLUSIONS

The results of the experimental studies presented in the last section support the view that the quadrustational system generally offers a higher degree of accuracy and reduces the elements of uncertainty as compared with the conventional two-station system. This was due to the fact that

- the number of degrees of freedom are increased, and
- any gross error can be easily detected.

Based on the theoretical and experimental studies in this paper, it can be concluded that

- The accuracy is more homogeneous in all coordinate axes when using the quadrustational system as compared with the two-station system; and
- The system produces higher accuracy in the Z-direction, which is of paramount importance to most engineering measurement problems. Incorporation of optimization principles into the system, to determine the optimal point, has the following advantages: (a) the optimal point (P in Figure 3) represents an acceptable point for the location of intersection of the four rays involved in the quadrustational system; (b) the system is reduced to a 3 by 3 matrix, while eight equations are for-

mulated for a simultaneous vector intersection; and (c) most of the available minicomputers can execute the simultaneous solution of the quadrustational system to determine the optimal point.

References

Abdel-Aziz, Y. I., and H. M. Karara, 1971. Direct Linear Transformation from Comparator Coordinates into Object Space Coordinates in Close-Range Photogrammetry. *Proceedings of the ASP Symposium on Close-Range Photogrammetry*, Urbana, Illinois.

Faig, W., 1972. Single Camera Approaches in Close-Range Photogrammetry. *Proceedings of the 38th Annual ASP Meeting*, Washington, D.C.

Granshaw, S. I., 1980. Bundle Adjustment Methods in Engineering Photogrammetry. *Photogrammetric Record* 10(56):181-203.

Hottier, P., 1976. Accuracy of Close-Range Analytical Restitution: Practical Experiments and Prediction. *Photogrammetric Engineering* 42(3):345-375.

Karara, H. M., 1968. *On the Precision of Stereometric System.* Civil Engineering Studies, Photogrammetric Series No. 14, University of Illinois.

———, 1974. "Recent Developments and Trends in Close-Range Photogrammetry." Invited Paper, First Pan-American and Third National Congress of Photogrammetry, Photo-Interpretation and Geodesy, Mexico City.

Kenefick, J. F., 1971. Ultra-Precise Analytics. *Photogrammetric Engineering*, 37(11):1167-1187.

Okamoto, A., 1981. Orientation and Construction of Models. Part I: *Photogrammetric Engineering and Remote Sensing*, 47(10):1437-1454.

———, 1981. Orientation and Construction of Models. Part II: *Photogrammetric Engineering and Remote Sensing*, 48(11)1615-1626.

Thompson, E. H., 1971. Space Resection without Interior Orientation. *Photogrammetric Record*, 7(37).

Wong, K. W., 1975. Mathematical Formulation and Detail Analysis in Close-Range Photogrammetry. *Photogrammetric Engineering and Remote Sensing*, 41(11).

(Received 27 March 1982; revised and accepted 7 November 1983)

Forthcoming Articles

Fouad A. Ahmed, Photogrammetric Application of a Video System in Three-Dimensional Recording.

C. Lisette Dottavio and *F. Dominic Dottavio*, Potential Benefits of New Satellite Sensors to Wetland Mapping.

Thomas D. Frank, Assessing Change in the Surficial Character of a Semiarid Environment with Landsat Residual Images.

John G. Gergen, The Geodetic Basis for Precise Photogrammetric Densification.

Soren W. Henriksen, Photogrammetric Geodesy Over Large Regions.

James R. Lucas, Photogrammetric Densification of Control in Ada County, Idaho: Data Processing and Results.

Stephen A. Mundy, Evaluation of Analytical Plotters for the Commercial Mapping Firm.

Leslie H. Perry, Photogrammetric Summary of the Ada County Project.

A. O. Quinn, Legal Aspects of Photogrammetric Measurements for Surveying and Mapping.

Steven L. Richardson, Pioneers and Problems of Early American Photogrammetry.

W. D. Rosenthal and *B. J. Blanchard*, Active Microwave Responses: An Aid in Improved Crop Classification.

William P. Tayman, User Guide for the USGS Aerial Camera Report of Calibration.

Manmohan M. Trivedi, Clair L. Wyatt, David R. Anderson, and *Howard T. Voorheis*, Designing a Deer Detection System Using a Multistage Classification Approach.

E. Vozikis, Some Theoretical and Practical Aspects of the OR1/SORA-PR System.